remote sensing

Article

A UAS and Machine Learning Classification Approach to Suitability Prediction of Expanding Natural Habitats for Endangered Flora Species

Mladen Jurišić, Dorijan Radočaj *, Ivan Plaščak and Irena Rapčan

Faculty of Agrobiotechnical Sciences Osijek, Josip Juraj Strossmayer University of Osijek, Vladimira Preloga 1, 31000 Osijek, Croatia; mjurisic@fazos.hr (M.J.); iplascak@fazos.hr (I.P.); irapcan@fazos.hr (I.R.)

* Correspondence: dradocaj@fazos.hr; Tel.: +385-31-554-879

Abstract: In this study, we propose integrating unmanned aerial systems (UASs) and machine learning classification for suitability prediction of expanding habitats for endangered flora species to prevent further extinction. Remote sensing imaging of the protected steppe-like grassland in Bilje using the DJI P4 Multispectral UAS ensured non-invasive data collection. A total of 129 individual flora units of five endangered flora species, including small pasque flower (*Pulsatilla pratensis* (L.) Miller ssp. *nigricans* (Störck) Zämelis), green-winged orchid (*Orchis morio* (L.)), Hungarian false leopardbane (*Doronicum hungaricum* Rchb.f.), bloody cranesbill (*Geranium sanguineum* (L.)) and Hungarian iris (*Iris variegate (*L.)) were detected and georeferenced. Habitat suitability in the projected area, designated for the expansion of the current area of steppe-like grassland in Bilje, was predicted using the binomial machine learning classification algorithm based on three groups of environmental abiotic criteria: vegetation, soil, and topography. Four machine learning classification methods were evaluated: random forest, XGBoost, neural network, and generalized linear model. The random forest method outperformed the other classification methods for all five flora species and achieved the highest receiver operating characteristic (ROC) values, ranging from 0.809 to 0.999. Soil compaction was the least favorable criterion for the habitat suitability of all five flora species, indicating the need to perform soil tillage operations to potentially enable the expansion of their coverage in the projected area. However, potential habitat suitability was detected for the critically endangered flora species of Hungarian false leopardbane, indicating its habitat-related potential for expanding and preventing further extinction. In addition to the current methods of predicting current coverage and population count of endangered species using UASs, the proposed method could serve as a basis for decision making in nature conservation and land management.

Keywords: nature conservation; random forest; environmental criteria; classification; multispectral imaging

Citation: Jurišić, M.; Radočaj, D.; Plaščak, I.; Rapčan, I. A UAS and Machine Learning Classification Approach to Suitability Prediction of Expanding Natural Habitats for Endangered Flora Species. *Remote Sens.* **2022**, *14*, 3054. https://doi.org/10.3390/rs14133054

Academic Editors: Pablo Rodríguez-Gonzálvez and Eben Broadbent

Received: 12 May 2022
Accepted: 24 June 2022
Published: 25 June 2022

1. Introduction

In recent years, and especially after the accession of the Republic of Croatia to the European Union, there have been significant changes in the needs related to environmental monitoring and management in Croatia. These changes primarily include: (1) greater importance to the aspect of nature protection, for which the main instrument is the European ecological network Natura 2000 [1] and (2) the need for a detailed evaluation of environmental and natural resources, especially water, air, and soil, given the expected consequences of climate change [2]. The loss of natural habitats due to climate change, intensive agricultural production, drainage of wetlands, urban development, and environmental contamination are the main reasons for endangering various flora species worldwide [3,4]. In order to monitor the status and protection of flora, the International Union for Conservation of Nature (IUCN) has prescribed rules and criteria for assessing the endangerment of wild species and has set standards for the preparation of red lists [5].

All these conditions place additional demands on land management of protected natural areas in Croatia; under the new circumstances, a detailed inventory is required for the purpose of spatial planning [6]. The most recent study, in 2016, on the flora of the steppe-like grassland in Bilje reported a total of 109 plant species detected from 35 families [7]. The steppe-like grassland in Bilje was protected in 2001 under the category of natural monument and it represents an integral part of the ecological habitat network of the Republic of Croatia within the Natura 2000 [7]. Due to the human-made habitat degradation caused by suboptimal land management over the years, an initiative was started for the expansion of steppe-like grassland in Bilje. To perform such a procedure, due to the narrow ecological gradients of the present flora species, an accurate evaluation of the habitat suitability according to relevant abiotic factors is necessary [8]. These abiotic factors generally include climate, soil, and topography environmental components, which are continuously interacting with vegetation [9].

Among the previously detected flora species in Bilje's steppe-like grassland, there are five endangered flora species that are protected by the nature protection acts of Croatia [10]. These are small pasque flower (*Pulsatilla pratensis* (L.) Miller ssp. *nigricans* (Störck) Zämelis), green-winged orchid (*Orchis morio* (L.)), Hungarian false leopardbane (*Doronicum hungaricum* Rchb.f.), bloody cranesbill (*Geranium sanguineum* (L.)), and Hungarian iris (*Iris variegata* (L.)) [10,11]. The small pasque flower is a perennial herbaceous plant and a geophyte [12], which, at the beginning of the 1990s, had the status of a regionally extinct (RE) species in Croatia [12]. It was detected again, later in the decade, but still has the status of a critically endangered species and is strictly protected in Croatia. The green-winged orchid is a perennial herbaceous plant and a geophyte [13], which is found in pastures and grasslands individually or in small groups throughout Central and Southern Europe [13]. The Hungarian false leopardbane is a perennial herbaceous plant and a hemicryptophyte [14], which specifically inhabits dry grasslands, with the steppe-like grassland in Bilje being its only habitat in Croatia. The bloody cranesbill is a perennial herbaceous plant and a hemicryptophyte, which grows in dry, moderately acidic soils, as well as in sunny to semi-shady locations [15]. The Hungarian iris is a perennial herbaceous plant and a geophyte, specific for its narrow ecological valence regarding topographic conditions [16].

The conventional approach to habitat suitability studies include subjective methods with marginal reproducibility as they are dominantly affected by expert assumptions. Geographic information system (GIS)-based multicriteria anaylsis in combination with individual weight determination methods, such as analytic hierarchy procedure, enables flexible suitability calculations but is deficient with regard to computational efficiency and reliability [9]. To overcome these limitations while maintaining flexibility and straightforwardness in spatial prediction, machine learning methods have been increasingly adopted in habitat suitability analyses [17]. Since this approach requires a number of input enviromental criteria, the role of remote sensing imaging becomes even more valuable in serving as a fundamental data source. Due to the sensitivity of endangered flora species and the need to not affect their natural habitat, remote sensing imaging methods are particularly suitable for habitat suitability prediction and nature conservation in general [18,19]. Moreover, remote sensing imaging in red-edge and near-infrared spectral bands is sensitive to plants' photosynthetic activities that might vary over time [20]. It enables the detection of minor variabilities in vegetation properties of endangered flora species, as well as of vegetation in general, providing the reliability and robustness of suitability predictions [21]. To provide an efficient multispectral imaging solution with high spatial resolution in restricted locations, unmanned aerial systems (UASs) have been successfully implemented in various nature conservation studies, specifically ensuring non-invasive data collection in sensitive study areas [22]. Various machine learning classification algorithms have recently been established as state-of-the-art methods for suitability prediction in various disciplines, such as agriculture [9], forestry [23], nature and environment conservation [24], including land and marine contamination studies [25,26]. While these methods have been successfully utilized in previous studies [27,28], habitat suitability prediction methods according to environmental criteria have been relatively unexplored, especially for the purpose of extending the habitat of endangered flora species [29].

The aim of this study was to propose and evaluate a method for habitat suitability prediction of endangered steppe flora species based on UAS imaging and machine learning classification, which could be applied as a nature conservation decision-making tool at micro-scale locations. The proposed method is based on a thorough spatial analysis of relevant environmental spatial criteria (vegetation, soil, and topography) in GIS, which is used in land management activities in Croatia.

2. Materials and Methods

2.1. Study Area and Fieldwork

The steppe in Bilje is located in the central part of a cemetery and covers an area of 0.63 ha, representing the last remnant of the steppe-like grassland in Croatia (Figure 1). There is a significant share of the xerothermic elements from the eastern European steppes, for which this study area represents a westernmost limit of distribution [7]. Research in the past thirty years has confirmed that there were more such habitats in eastern Croatia but they have mostly disappeared due to land-use transformation into arable land or overgrowing with shrubs [10].

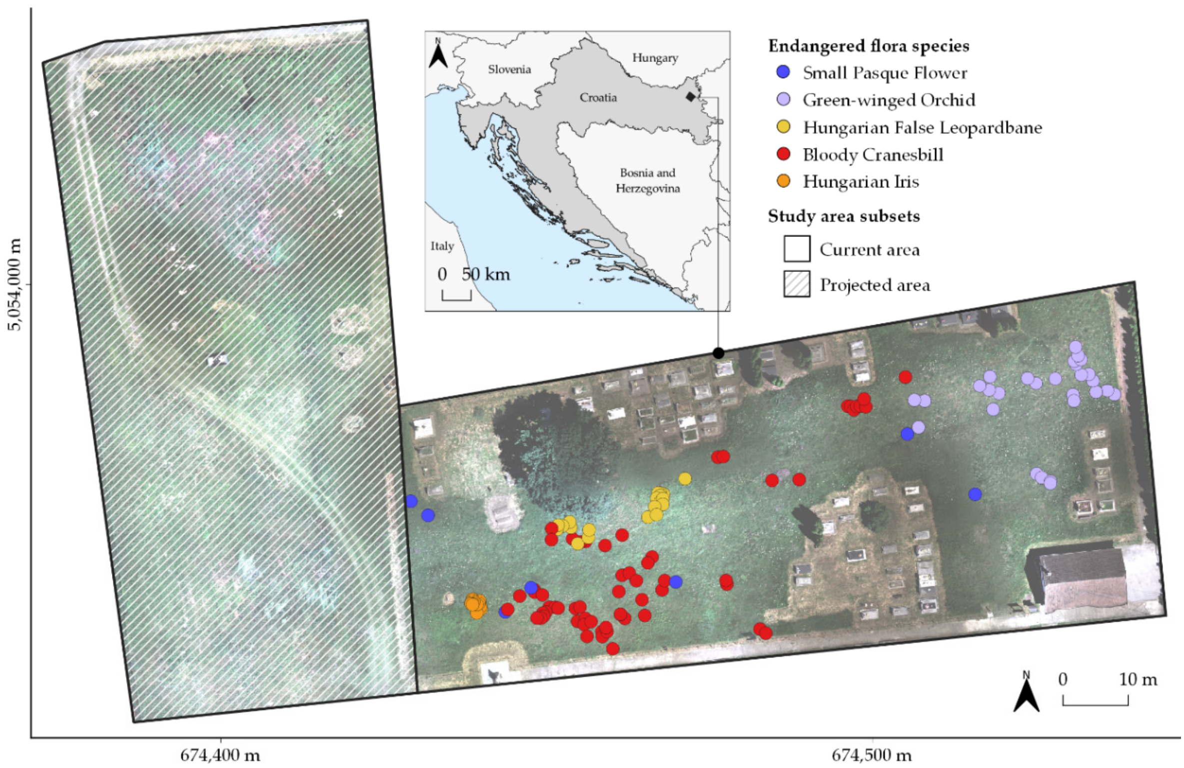

Figure 1. The current and projected areas of steppe-like grassland in Bilje with locations of detected flora species.

Data collection in the steppe-like grassland in Bilje was carried out in ten iterations during 2021: 28 January, 15 February, 1 March, 18 March, 30 March, 14 April, 30 April, 14 May, 1 June, and 14 June 2021 (Figure 2). A DJI P4 Multispectral UAS was used for the remote sensing imaging in the blue (B), green (G), red (R), red-edge (RE), and near-infrared (NIR) spectral bands. The imaging for all iterations was performed using the same mission and parameters, with 35 m relative altitude, 4.0 m s^{-1} fight speed, 80% front overlap, 70% side overlap, and imaging at nadir angle. The images were directly georeferenced based on the Global Navigation Satellite System (GNSS), using the Croatian Positioning System (CROPOS) Very-High Precision Positioning (VPPS) service, which enabled positioning accuracy of 2 cm horizontally and 4 cm vertically [30]. The digital orthophoto and digital surface model were created in the Agisoft Metashape Professional software v1.5.2 (St. Petersburg, Russia), based on the structure-from-motion process from dense point cloud. A digital orthophoto was created for each of the imaging sets with a spatial resolution of 2.0 cm from the 1.9 cm ground sample distance, processed as the multispectral image band stack. The digital surface model used for calculations of the topographic indicators of microrelief was determined using UAS imagery sensed on 28 January 2021 with a spatial resolution of 7.5 cm, when canopy height was at its lowest in the study period. Soil sampling was performed using an Eijkelkamp soil and water penetrometer at 72 randomly selected soil samples distributed across the study area.

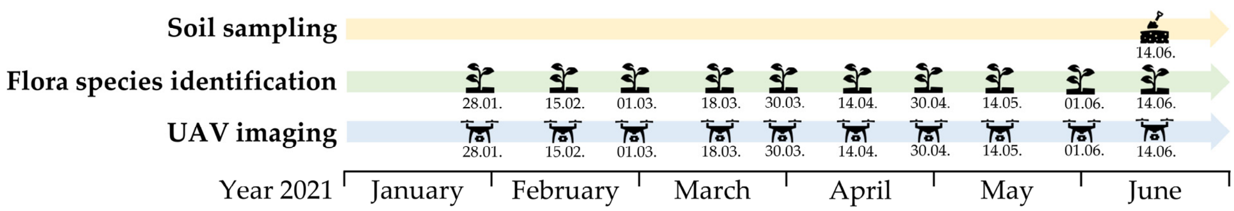

Figure 2. The timeline of the performed fieldwork at the steppe-like grassland in Bilje, during 2021.

A total of 129 individual flora units across the study area were identified in the field and georeferenced (Table 1, Figure 3). A Trimble R8s global navigation satellite system (GNSS) receiver was used for the real-time kinematic (RTK) georeferencing, using the CROPOS VPPS service. The IUCN classes representing vulnerability on the national level were evaluated in the Flora Croatica database [11]. Among the evaluated existing flora species, the vulnerability classes consisted of critically endangered (CR), endangered (EN), vulnerable (VU), near threatened (NT), and least concern (LC).

Table 1. Endangered flora species detected during the fieldwork.

English Name	Latin Name	Family	IUCN Class	Units Detected
Small pasque flower	*Pulsatilla pratensis* (L.) Miller ssp. *nigricans* (Störck) Zämelis	*Ranunculaceae*	CR	7
Green-winged orchid	*Orchis morio* (L.)	*Orchidaceae*	NT	29
Hungarian false leopard-bane	*Doronicum hungaricum* Rchb.f.	*Asteraceae*	CR	20
Bloody cranesbill	*Geranium sanguineum* (L.)	*Geraniaceae*	LC	61
Hungarian iris	*Iris variegata* (L.)	*Iridaceae*	NT	12

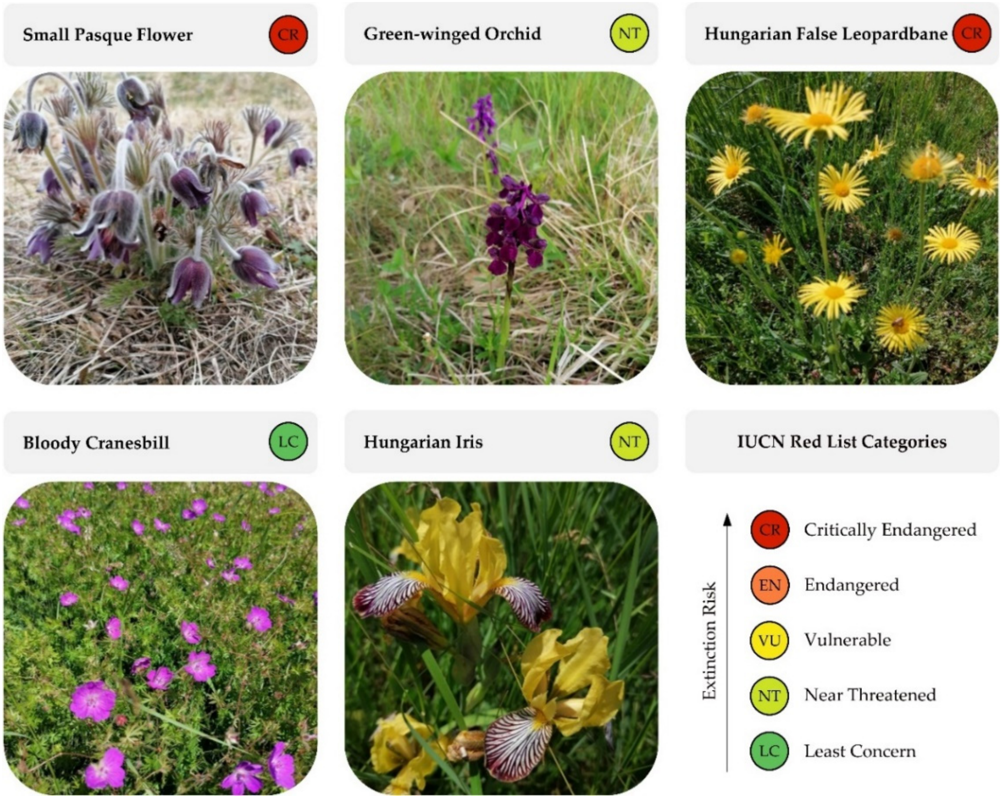

Figure 3. Images of the detected endangered flora species.

2.2. Spatial Modeling of Environmental Criteria

The habitat suitability prediction of endangered steppe flora species in Bilje's steppe-like grassland was performed using three groups of independent environmental criteria: vegetation, soil, and topography. These criteria groups have been commonly used in spatial predictions, as the most relevant environmental criteria [31]. While these criteria groups represent structural ecosystem parameters [32], only those criteria which showed variability in the study area were selected for suitability prediction. Although climate conditions are among the recommended criteria [31], the variability of climate conditions over the study area could not be quantified due to sparse spatial resolution of available climate data [33]. Spearman correlation coefficients were used to determine the mutual relationships of individual environmental covariates. The spatial modeling of environmental criteria was performed using the open-source GIS software SAGA GIS v7.3.0 (Göttingen, Germany) [34], which was georeferenced in the Croatian Terrestrial Reference System (HTRS96/TM, EPSG: 3765).

2.2.1. Vegetation Criteria

The vegetation criteria included vegetation indices derived from multitemporal UAS imaging, that allowed the assessment of biophysical vegetative properties, such as chlorophyll content [35]. Two vegetation indices were selected to represent vegetation criteria, i.e., the normalized difference vegetation index (NDVI) [36] and the normalized difference red-edge index (NDRE) [37]. Their calculation was performed according to Equations (1) and (2) as follows:

$$\mathrm{NDVI} = \frac{\mathrm{NIR} - \mathrm{R}}{\mathrm{NIR} + \mathrm{R}}, \quad (1)$$

$$\mathrm{NDRE} = \frac{\mathrm{RE} - \mathrm{R}}{\mathrm{RE} + \mathrm{R}}. \quad (2)$$

These are the two of the most well-known and globally documented vegetation indices, with very wide application and high accuracy in monitoring the properties of vegetation in previous studies [38–40]. The differences of vegetation indices over the study period were evaluated using the paired *t*-test, calculated from all combinations of consecutive NDVI and NDRE observations.

2.2.2. Soil Criteria

Soil criteria included the physical parameter of soil compaction determined by using a soil penetrometer at a discrete set of locations, since it was the only soil property which was determined to be heterogeneous in the study area. Soil compaction, as a limiting factor in the development of the root system of endemic flora species [41], was selected as an indicator of the physical component of soil suitability. Soil compaction was sampled at three soil depths: 0–5 cm, 5–10 cm, and 10–15 cm, which included vertical soil stratification of the utmost importance for the development of the root system of detected flora species [11]. Spatial interpolation of soil compaction in the entire study area was performed by geostatistical data processing using the inverse distance weighting interpolation method with a power parameter of 2 due to the lack of spatial autocorrelation, normality, and stationarity of input data, as was recommended in previous studies [42,43].

2.2.3. Topographic Criteria

Topographic criteria were calculated in the GIS environment based on the application of empirical algorithms of the digital relief model values [44]. The topographic parameters of digital surface model, slope, total potential annual insolation, and flow accumulation were selected as the main indicators of microrelief, according to their complimentary representation of topographic properties [44,45]. The terrain slope and the flow accumulation model were specifically selected to model water retention in soil after precipitation [46], according to moderate depressions in the central part of the current coverage of the steppe-like grassland. The flow accumulation was calculated using the multiple flow direction method with a top-down process and sink removal in preprocessing [47]. The total potential annual insolation is a fundamental indicator of the impact of microrelief on the availability of sunlight [48], providing mutually complementary information to the aforementioned indicators.

2.3. Habitat Suitability Prediction Using Machine Learning

The aggregated suitability of the study area for endangered flora species was determined by supervised binomial classification methods, and included evaluation of the random forest, XGBoost, neural network, and generalized linear model methods. The most accurate method was selected for each of the individual flora species, based on the highest receiver operating characteristic (ROC) value, with displayed sensitivity and specificity as its components. The optimal parameters of the machine learning classification methods were determined on the iterative basis, using the combination of parameters which produced the highest ROC values as the most accurate variant. Machine learning classification and accuracy assessment were performed using R x64 v4.0.3 in RStudio v2021.09.2 (Boston, MA, USA) with “caret” library [49]. The prediction was performed with all three groups of environmental criteria (vegetation, topography, and soil). Training samples consisted of georeferenced locations of flora species detected in the field for the individual species, combined with the 27 random samples, to match the number of input environmental covariates. The random samples were generated with 10 m mutual distance and at least 2 m from the nearest flora unit. The number of training data varied according to the number of detected flora units, as displayed in Table 1. The total number of training data was 88 for bloody cranesbill, 56 for green-winged orchid, 39 for Hungarian iris, 47 for Hungarian false leopardbane, and 34 for small pasque flower. The classification results included two classes: one class, representing area with higher suitability for flora species relative to the random locations in the study area and a second class, representing presently non-suitable area. The variable importance was determined for each classification variant per flora species, quantifying the scaled variable importance with the maximum value of 100. The proposed habitat suitability prediction method for endangered flora species is summarized in Figure 4.

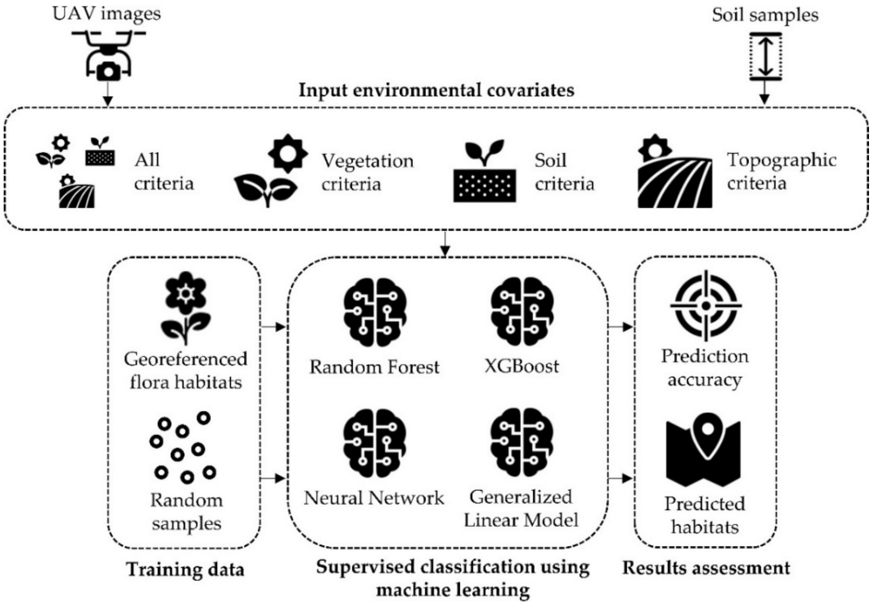

Figure 4. The proposed method for habitat suitability prediction based on unmanned aerial vehicle remote sensing and machine learning classification.

3. Results

The results of paired *t*-test from all combinations of consecutive NDVI and NDRE observations are presented in Table 2. The spectral signatures of detected flora species, as mean values per spectral band in five bands are shown in Appendix A. A period of smaller changes in the values of the vegetation indices (until 12 April 2021), and then an increase in the indices and higher variability caused by latter growth stages of flora species (after 12 April 2021) were observed (Figure 5). The vegetation criteria represented by the NDVI and NDRE vegetation indices resulted in individual value spikes for the majority of the observed flora species, which could be differentiated from the rest of the study area. The largest increases in vegetation indices as compared with the previous observations occurred for Hungarian false leopardbane and Hungarian *Ir*is on 30 April 2021, as well as for green-winged orchid and small pasque flower on 1 June 2021.

Table 2. The results of the paired *t*-test from all combinations of consecutive NDVI and NDRE observations.

First Observation	Second Observation	NDVI		NDRE	
		t	*p*	t	*p*
28 January 2021	15 February 2021	5.2524	<0.0001	5.8283	<0.0001
15 February 2021	1 March 2021	2.1964	0.0290	0.9416	0.3472
1 March 2021	18 March 2021	−2.9588	0.0034	−2.7005	0.0074
18 March 2021	30 March 2021	−2.8197	0.0052	−4.9542	<0.0001
30 March 2021	12 April 2021	−6.4170	<0.0001	−7.021	<0.0001
12 April 2021	30 April 2021	−1.6302	0.1043	−0.5633	0.5737
30 April 2021	14 May 2021	−5.8383	<0.0001	−6.2335	<0.0001
14 May 2021	01 June 2021	0.6704	0.5032	0.9132	0.3620
01 June 2021	14 June 2021	9.0903	<0.0001	9.9859	<0.0001

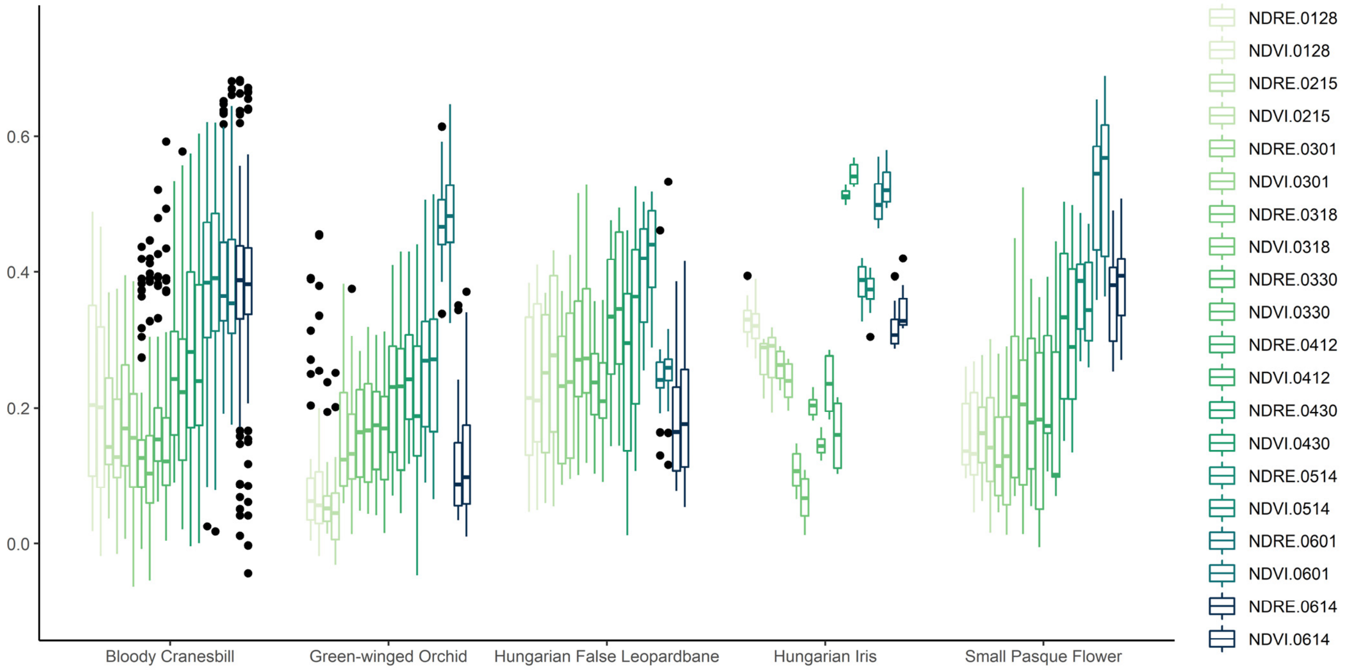

Figure 5. Boxplots of the NDVI and NDRE vegetation indices in the study period (black dots represent outliers).

Overall, the study area showed a wide range of values for all four topographic criteria. The current habitats of the endangered flora species showed narrow value ranges up to 0.30 of the normalized value interval, representing the ecological valence of individual species (Figure 6). The topographic criteria indicated the presence of two distinct features within the study area: a depression in the central part of the current area of Bilje's steppe-like grassland and a hill in the northern part of the projected area (Figure 7). The habitats of observed species mutually differentiated primarily in the elevation from the digital surface model and total potential insolation values. Particular species had very distinct topographic properties, including elevation of Hungarian iris and Hungarian false leopardbane, as well as the total potential insolation for Hungarian iris.

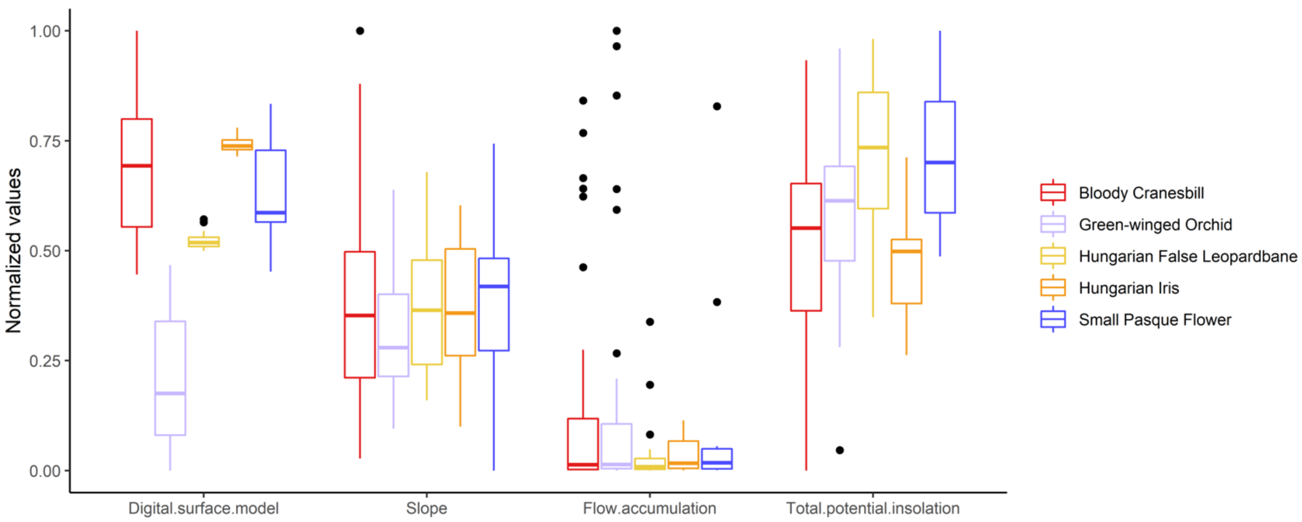

Figure 6. Boxplots of topographic indices per flora species (black dots represent outliers).

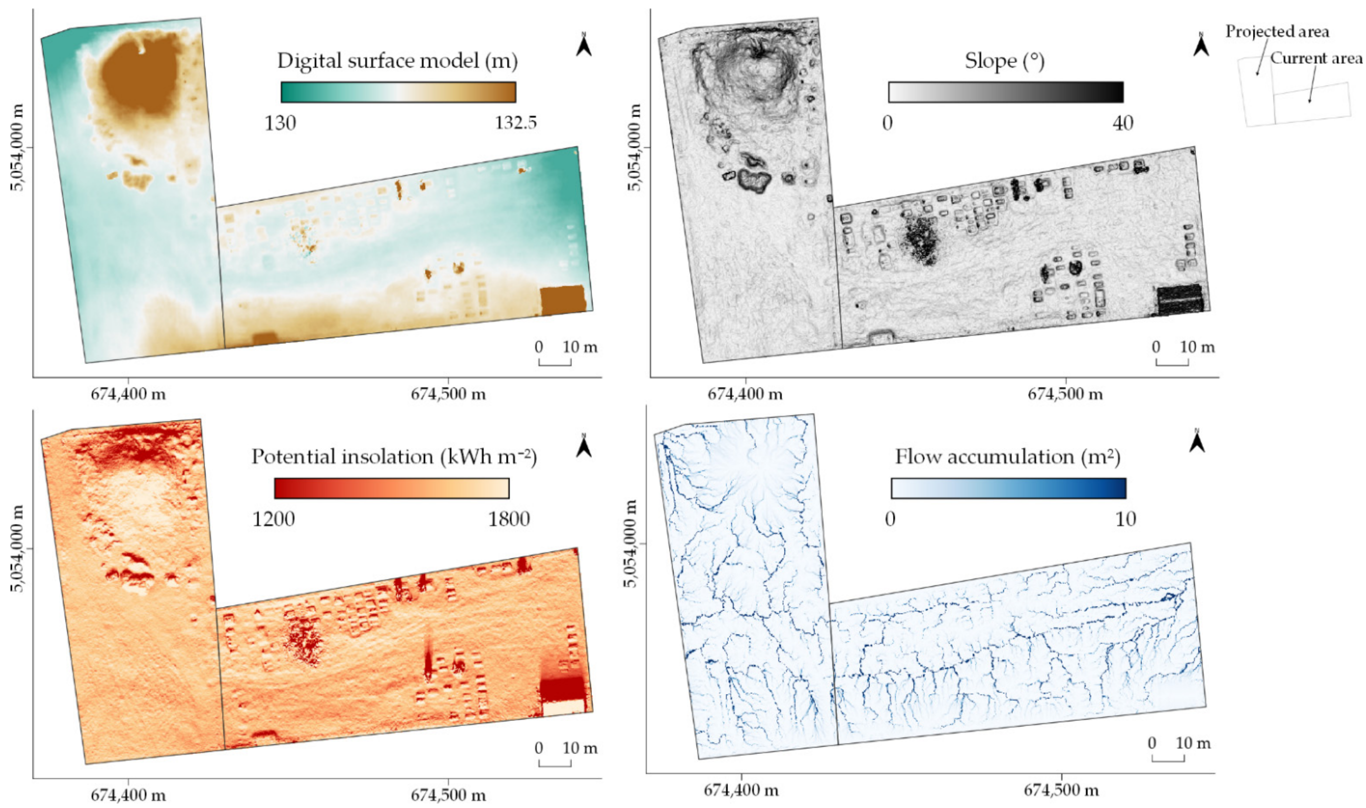

Figure 7. The four components of the topographic criteria group.

The average soil compaction values of the current flora species habitats were in line with the general value distribution in the current area (Figure 8), while Hungarian iris had noticeably lower soil compaction values than other species in all three soil layers. While the majority of considered soil properties had no significant variability in the study area, soil compaction values resulted in very high value ranges (Figure 9). The current area of the steppe-like grassland in Bilje had continuously low soil compaction in the upper soil layer, with a gradual increase in soil compaction in deeper soil layers. However, the projected area had two distinct areas with extreme soil compaction values regardless of soil depth, i.e., very low soil compaction in the hilly section in the northern part and very high soil compaction in the southern part.

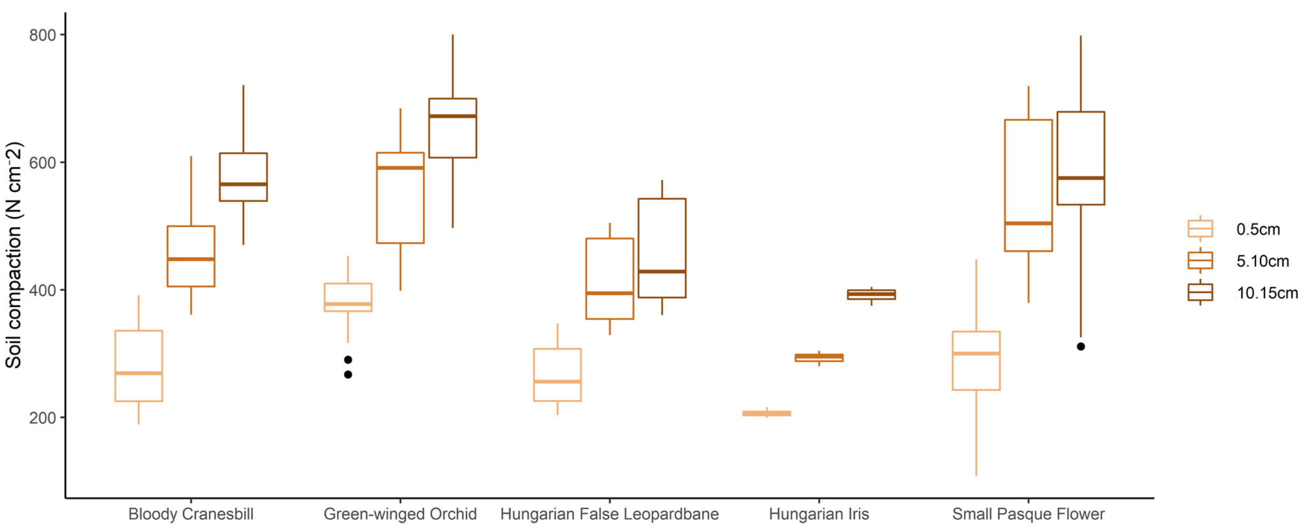

Figure 8. Boxplots of soil compaction at three soil depth layers per flora species (black dots represent outliers).

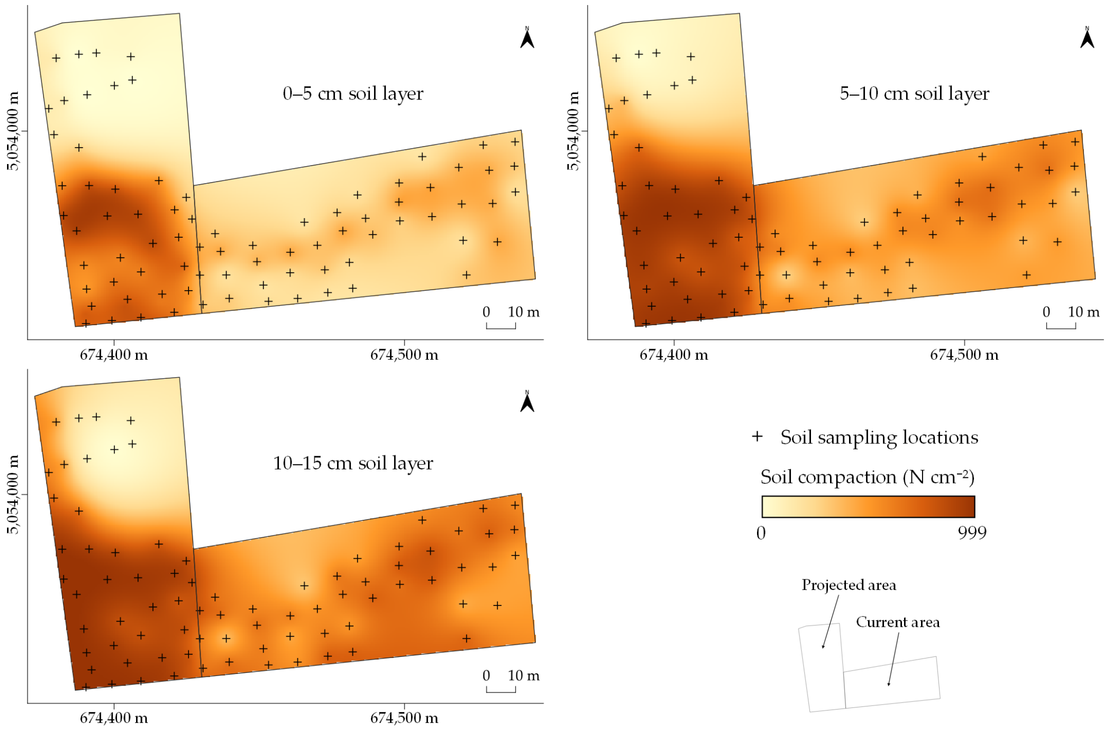

Figure 9. The soil compaction at three soil depth layers.

Overall, the vegetative criteria had positive mutual correlations during the entire study period, especially during late March and mid-April (Figure 10). While the value ranges of soil compaction were distinct relative to the soil depth layers, their values increased proportionally with soil depth, resulting in a high positive correlation. The digital surface model and terrain slope had negative correlations with total potential insolation and flow accumulation, indicating complimentary information regarding the microrelief. Individual criteria from the vegetation, soil, and topography criteria groups produced no positive correlation for any combination of the individual criteria.

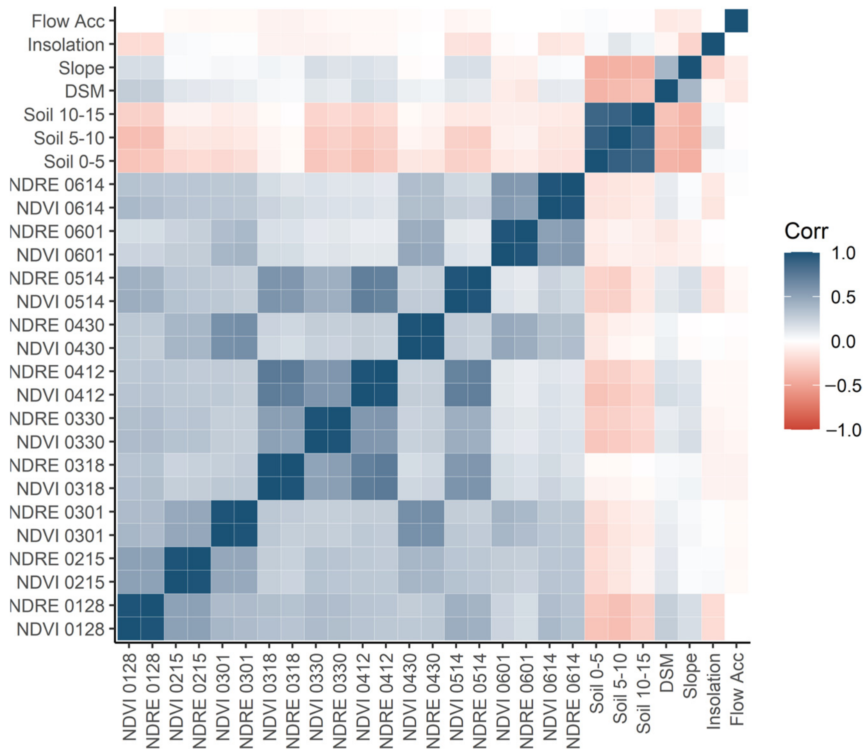

Figure 10. The correlation plot for input environmental criteria.

The binomial classification accuracy per flora species is presented in Table 3. The random forest method produced superior classification accuracy relative to the evaluated machine learning methods for all five flora species, closely followed by XGBoost in four cases. Flora species with the lowest number of input samples, i.e., small pasque flower and Hungarian iris, produced the lowest and the highest classification accuracy, respectively.

Table 3. Accuracy assessment of binomial classification per flora species.

Flora Species	Metric	Random Forest	XGBoost	Neural Network	Generalized Linear Model
Bloody cranesbill	ROC	**0.964**	0.956	0.914	0.694
	Sensitivity	0.567	**0.617**	0.517	0.500
	Specificity	**0.967**	0.933	0.902	0.883
Green-winged orchid	ROC	**0.967**	0.956	0.922	0.964
	Sensitivity	**0.900**	0.817	0.683	0.783
	Specificity	0.933	0.933	0.867	**0.967**
Hungarian false leopardbane	ROC	**0.999**	0.967	0.958	0.825
	Sensitivity	**0.967**	0.933	0.733	0.633
	Specificity	**0.950**	0.900	**0.950**	0.900
Hungarian iris	ROC	**0.999**	**0.999**	**0.999**	0.850
	Sensitivity	**0.999**	0.950	0.867	0.650
	Specificity	**0.999**	**0.999**	**0.999**	**0.999**
Small pasque flower	ROC	**0.809**	0.738	0.762	0.607
	Sensitivity	**0.933**	0.867	0.633	0.700
	Specificity	0.429	0.143	**0.857**	0.714

The most accurate results per classification are shown in bold.

The complete representation of the predicted habitat suitability is presented in Figure 11. The suitability levels of bloody cranesbill predominated, followed by Hungarian false leopardbane and green-winged orchid, indicating the presence of suitable environmental conditions. The small pasque flower and Hungarian iris resulted in narrow ecological variances of the observed criteria, which were met in a very limited part of the projected area of expansion.

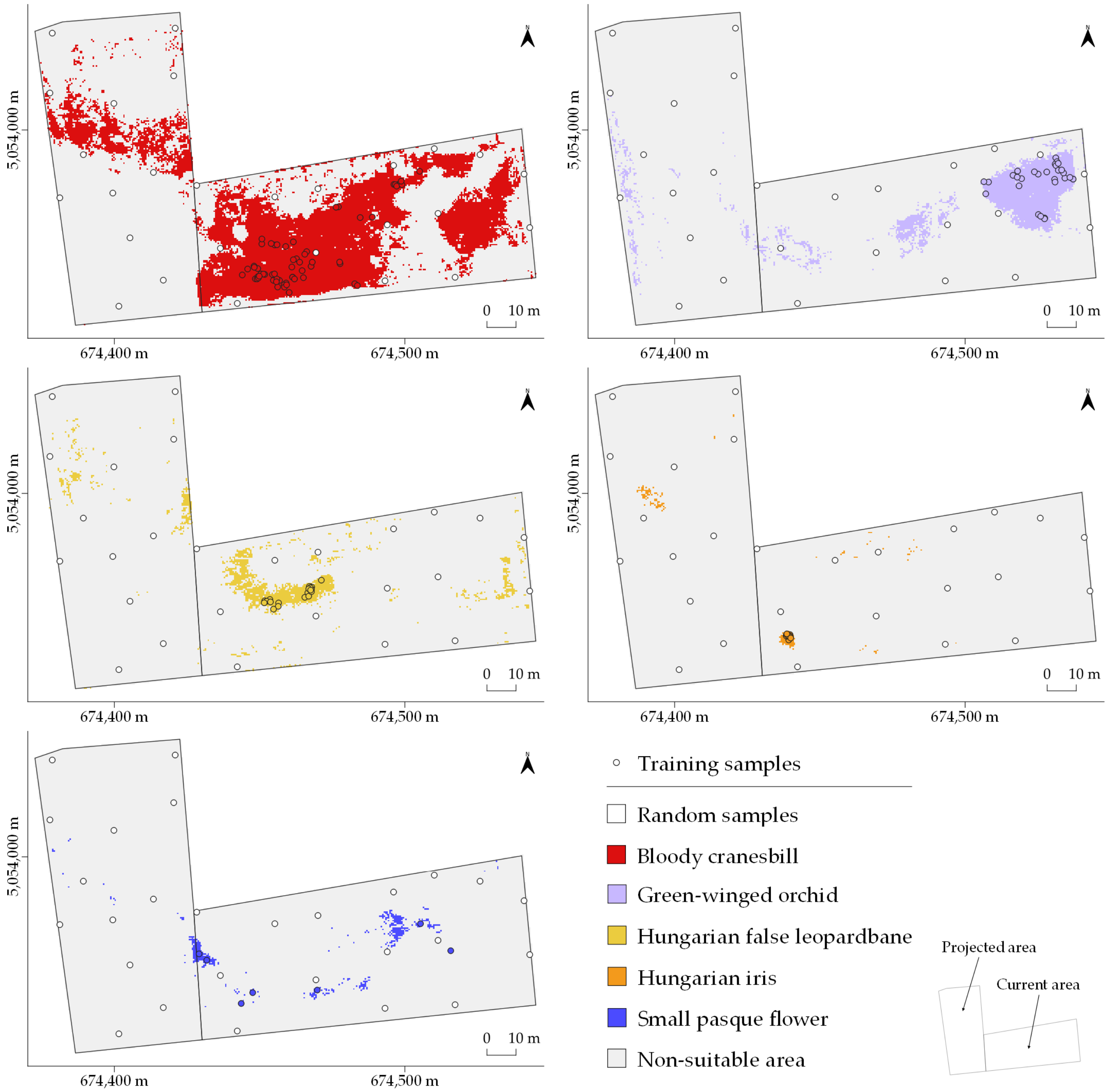

Figure 11. Display of predicted habitat suitability of the most accurate classification method per flora species.

The variable importance of classified suitability for five flora species indicated a wide range of crucial environmental criteria, as well as the UAS imaging periods (Figure 12). The random forest classification results, as the most accurate evaluated classification variant, were selected for the assessment of the variable importance. Vegetation indices dominated among the most important criteria for all flora species, especially those collected in late March and early to mid-June. Soil compaction was represented at all three soil depth layers, while total potential insolation and the digital surface model were the most important topographic criteria.

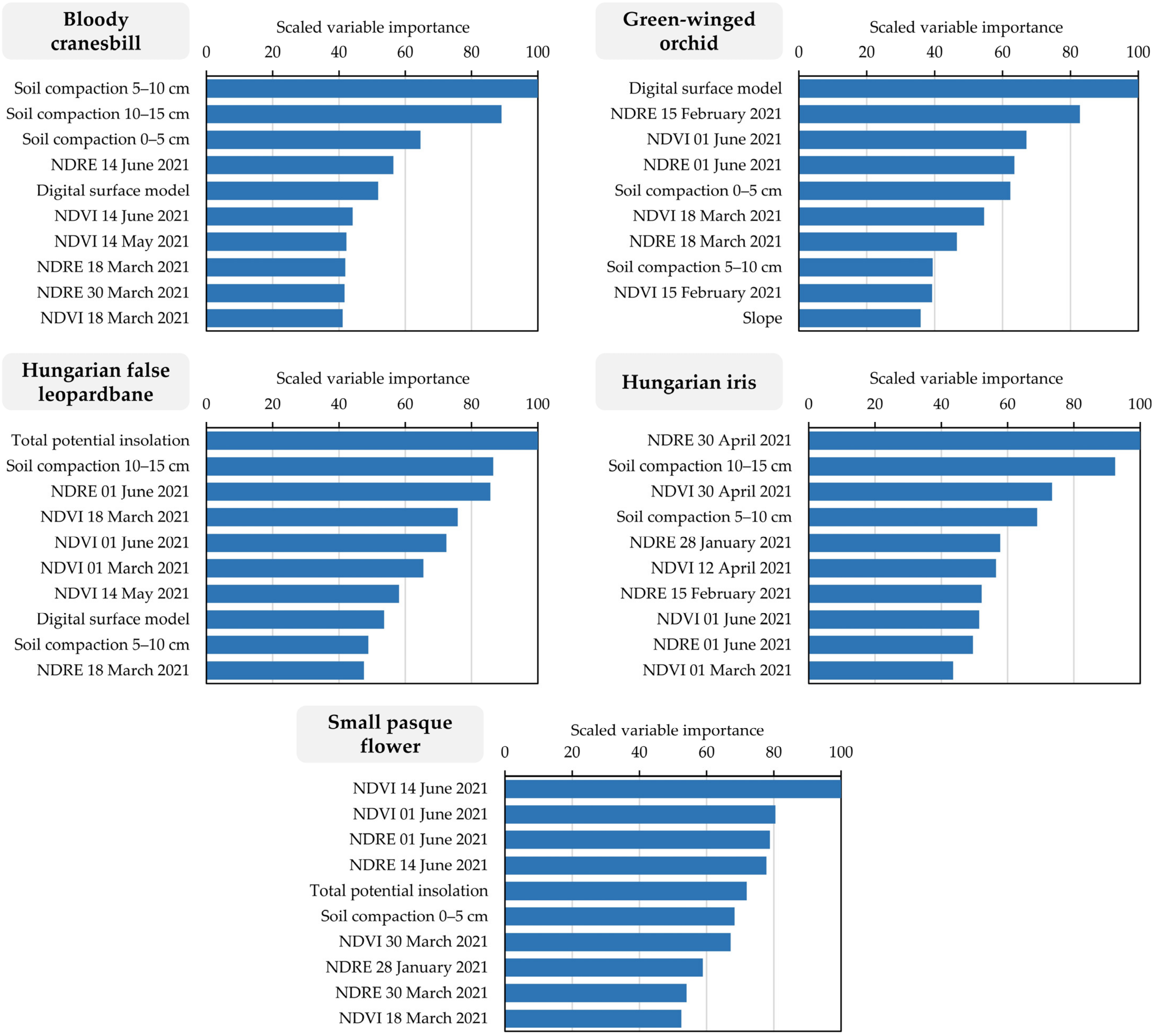

Figure 12. The top ten important variables of the most accurate classification method per flora species.

4. Discussion

The field detection of flora units from this study indicated an increase in the population count of endangered flora species, with the number of detected flora units increasing to 129 as compared with 109 units five years prior [7]. To potentially extend their habitat to neighboring areas, we proposed a habitat suitability prediction method based on non-invasive field observations from remote sensing imaginh using a UAS multispectral camera system and machine learning classification. Since the evaluated environmental conditions, including vegetation, soil, and topography criteria, impact the ecological gradient of both flora and fauna species [50–52], the proposed approach should be applicable to a wide variety of endangered species. Moreover, the application of the UAS mounted multispectral camera system ensured that flora and fauna species would be minimally disturbed in their natural habitat during the field observations and non-invasive population count [53]. However, the proposed suitability calculation approach presently does not include environmental conditions which are difficult to model in the GIS environment but are impactful on habitat suitability of flora species. These include random grazing or browsing by animals or soil invertebrate fauna [54].

The random forest classification method utilized the three groups of environmental criteria with the highest prediction accuracy. To include spatial data that would highlight the existing variability in the environmental conditions of the study area, the inclusion of additional remote sensing sensors could potentially upgrade the existing suitability results. In addition to the presently utilized multispectral sensors, previous research has indicated that hyperspectral sensors [55] and LiDAR [56] could provide supplementary spatial information of predominately structural environmental conditions and could be successfully integrated with machine learning classification methods. UASs have also ensured high prediction accuracy in related studies for nature conservation, such as flora species population count and coverage area prediction [57,58]. Although machine learning classification methods, such as those evaluated in this study, are generally resistant to overfitting which might occur in the process, overfitting still might occur due to exaggerated pruning [59]. Since the abovementioned studies focused on the detection of environmental conditions present during the data collection period, the proposed approach for habitat suitability prediction extends the present possibilities of land management for protected natural areas. The approach of integrating machine learning with multispectral images acquired using UASs has been proven to be successful regardless of the study area location at many other locations around the globe, with the only notable disadvantage of relatively small imaging coverage [60]. Due to the requirements of high imaging spatial resolution and flight altitude restrictions implemented by the majority of countries, this approach is likely to remain applicable only for smaller areas. For larger study areas, global open-data multispectral satellite missions and digital elevation models could be primary data sources that ensure a moderate spatial resolution [61]. However, these data do not allow any type of classification at the individual plant or herbaceous species level.

Although bloody cranesbill exhibited the highest ecological valence and distribution area among the studied flora species, three distinct sets of environmental criteria clearly had the highest importance. These criteria consisted of soil compaction across all soil depths, vegetation indices in mid-June, and the same indices in mid- to late March. While the observations in May and June coincide with the flowering period, with consequently rapid changes in spectral signatures, the importance of March observation implies the necessity of its further exploration in future studies. The green-winged orchid had similar criteria sets and respective time periods as that of the most important bloody cranesbill, with more emphasized topographic criteria of the digital surface model and the terrain slope. This observation aligns with their natural habitat in the study area, where it was found exclusively on flat terrain with lower elevation than their surroundings. Hungarian false leopardbane had the highest requirements for a narrow range of total insolation, as well as soil compaction at deeper soil layers. Vegetation criteria also had two distinct time periods which had the greatest effect on classification, which included March and early June. Contrary to the most important study periods of the bloody cranesbill, vegetation indices from the flowering period in April and early May did not have a major impact on the classification results. Although Hungarian iris was detected in a very small part of the study area in a minor terrain depression, as a very distinct section of the microrelief, no topographic criteria were among the most important variables. The vegetation indices with the greatest importance were collected over the entire study period, indicating that Hungarian iris requires fieldwork in regular study periods for its effective monitoring. The vegetation indices collected during late March and mid- to late June were among the most important variables for habitat suitability classification for the small pasque flower. As a flora species which was detected in the widest area among studies species, it also showed a dependency on total insolation and soil compaction in the uppermost soil layer.

The extension of potential habitat areas for the five observed endangered flora species produced varying results, regarding the individual species and environmental conditions in the study area. The predicted habitat suitability area for the endangered flora species was the highest for bloody cranesbill, being the only species in the LC category, which will likely remain due to its wide ecological optimum in the study area. Among the critically endangered species, Hungarian false leopardbane resulted in a suitability potential for expanding its habitat in the projected area, which is especially encouraged for both flora and fauna species in the CR category [62]. Since the existing habitats of Hungarian iris are grouped in a relatively small current area, as well as being the least represented species in the projected area, special attention should be placed on protecting it from further extinction. Soil compaction is a specific occurrence which is among the few abiotic components that can be affected by adopting soil tillage adjustment operations, unlike climate conditions or topography, that which require land management to fully adjust to these conditions without the possibility of altering them directly [63]. This indicates a positive impact of including environmental conditions in suitability analyses which can be altered by human activity, but should be approached with caution as it might negatively affect other flora species in the study area.

5. Conclusions

The habitat suitability analysis for endangered flora species of the protected natural monument steppe-like grassland in Bilje for the purpose of extending their coverage zone determined the presence of five endangered flora species: small pasque flower, green-winged orchid, Hungarian false leopardbane, bloody cranesbill, and Hungarian iris. Three groups of environmental criteria , i.e., inducing vegetation, soil, and topography, were all represented in the variable importance analysis, justifying their selection and ensuring a complimentary suitability analysis from various ecological aspects. The vegetation criteria included multitemporal values of complementary vegetation indices (NDVI and NDRE), which indicated the possibility of detecting eco-physiologically similar locations in the current and projected area of the steppe-like grassland in Bilje. The variable importance from the machine learning classification results enabled the selection of the most important time periods for UAS imaging for particular flora species, enabling additional insight into the importance of flora species' growth stages and more economical fieldwork planning in the future. The topography criteria of the microrelief analysis included the influence of terrain on the basic abiotic factors that determine the growth of plant species, emphasizing the influence of total potential insolation and the potential benefit of including additional complimentary indices. The soil criteria included the physical parameter of soil compaction at three soil depth layers, which enabled suitability assessment for all five flora species, regarding the required soil depth for root development. The random forest method outperformed the XGBoost, neural network and the generalized linear model methods in the binomial classification of suitability for evaluating all flora species. On the basis of the random forest results, the conclusions were made about the possibilities of extending the coverage area of the steppe-like grassland in Bilje. According to the predicted suitability levels, the habitat coverage of bloody cranesbill and green-winged orchid could be extended presently. The proposed method also has high potential for implementation in habitat suitability assessments of other flora species, since vegetation, soil, and topography conditions impact the ecological gradient for a variety of similar species.

Author Contributions: Conceptualization, D.R.; methodology, D.R.; software, D.R.; validation, M.J. and I.P.; formal analysis, M.J. and D.R.; investigation, M.J., D.R., I.P., and I.R.; resources, M.J., D.R., I.P., and I.R.; data curation, D.R.; writing—original draft preparation, D.R.; writing—review and editing, D.R.; visualization, D.R.; supervision, M.J., I.P., and I.R.; project administration, M.J.; funding acquisition, M.J., D.R., and I.P. All authors have read and agreed to the published version of the manuscript.

Funding: This research received no external funding.

Data Availability Statement: Not applicable.

Acknowledgments: This work was supported by the Faculty of Agrobiotechnical Sciences Osijek as a part of the scientific project "AgroGIT—technical and technological crop production systems, GIS and environment protection".

Conflicts of Interest: The authors declare no conflicts of interest.

Appendix A

Table A1. The spectral signatures of detected flora species, as mean values per spectral band in five bands, for imaging dates during year 2021.

Flora Species	Bands	Mean Digital Number (DN) Values Divided by a Maximum DN Value									
		28.01.	15.02.	01.03.	18.03.	30.03.	12.04.	30.04.	14.05.	01.06.	14.06.
Small pasque flower	B	0.198	0.198	0.175	0.210	0.208	0.181	0.134	0.119	0.094	0.111
	G	0.213	0.209	0.172	0.214	0.212	0.193	0.176	0.159	0.150	0.165
	R	0.193	0.186	0.159	0.183	0.180	0.164	0.134	0.108	0.101	0.130
	RE	0.242	0.265	0.220	0.255	0.265	0.256	0.246	0.213	0.246	0.211
	NIR	0.233	0.259	0.216	0.246	0.250	0.243	0.233	0.203	0.248	0.220
Green-winged orchid	B	0.231	0.224	0.206	0.199	0.189	0.170	0.141	0.124	0.091	0.132
	G	0.230	0.226	0.201	0.198	0.195	0.181	0.184	0.174	0.140	0.187
	R	0.217	0.223	0.187	0.178	0.181	0.161	0.154	0.130	0.103	0.190
	RE	0.267	0.252	0.253	0.238	0.250	0.240	0.248	0.223	0.283	0.235
	NIR	0.268	0.244	0.245	0.240	0.248	0.240	0.232	0.221	0.296	0.237
Hungarian false leopardbane	B	0.183	0.147	0.167	0.139	0.162	0.117	0.094	0.074	0.105	0.109
	G	0.199	0.160	0.166	0.150	0.193	0.155	0.134	0.150	0.199	0.178
	R	0.184	0.150	0.163	0.139	0.170	0.128	0.135	0.104	0.157	0.158
	RE	0.283	0.234	0.232	0.238	0.273	0.255	0.227	0.232	0.252	0.229
	NIR	0.291	0.253	0.239	0.244	0.267	0.266	0.275	0.252	0.259	0.235
Bloody cranesbill	B	0.198	0.178	0.175	0.213	0.219	0.167	0.135	0.105	0.093	0.111
	G	0.197	0.177	0.172	0.216	0.231	0.190	0.164	0.159	0.156	0.163
	R	0.164	0.155	0.159	0.191	0.201	0.155	0.134	0.116	0.108	0.112
	RE	0.248	0.222	0.221	0.252	0.293	0.262	0.239	0.251	0.249	0.236
	NIR	0.239	0.213	0.210	0.247	0.279	0.253	0.234	0.252	0.250	0.236
Hungarian iris	B	0.116	0.124	0.150	0.194	0.238	0.172	0.064	0.082	0.079	0.123
	G	0.145	0.143	0.167	0.195	0.228	0.197	0.140	0.191	0.142	0.211
	R	0.115	0.116	0.145	0.181	0.178	0.171	0.087	0.123	0.091	0.136
	RE	0.234	0.207	0.246	0.231	0.257	0.275	0.271	0.302	0.267	0.264
	NIR	0.232	0.209	0.236	0.212	0.229	0.235	0.300	0.296	0.279	0.283

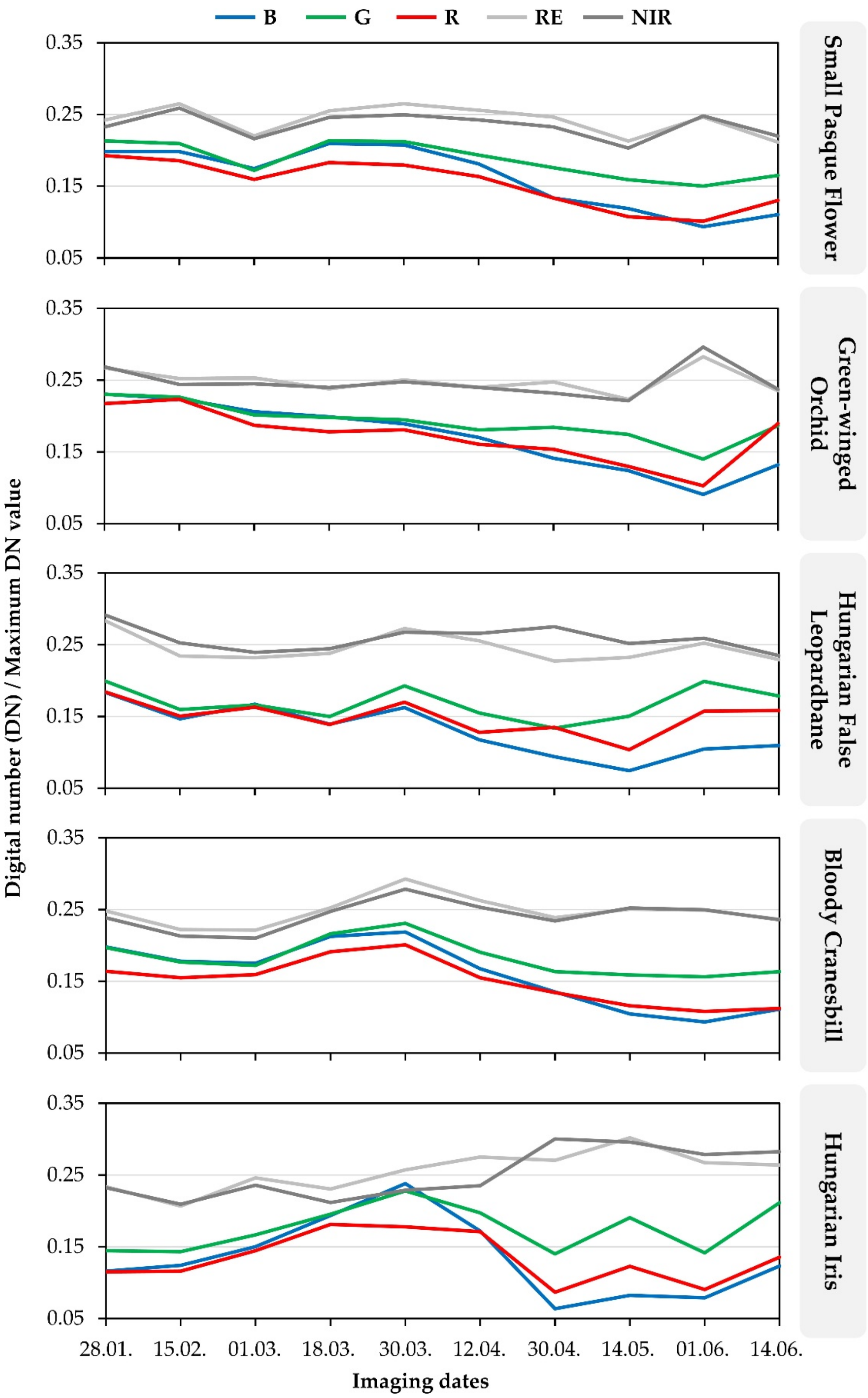

Figure A1. The display of the average spectral signatures of detected flora species in five spectral bands during the study period.

References

1. Biondi, E.; Casavecchia, S.; Pesaresi, S.; Zivkovic, L. Natura 2000 and the Pan-European Ecological Network: A New Methodology for Data Integration. *Biodivers. Conserv.* **2012**, *21*, 1741–1754. https://doi.org/10.1007/s10531-012-0273-7.
2. Bhatti, A.Z.; Farooque, A.A.; Li, Q.; Abbas, F.; Acharya, B. Spatial Distribution and Sustainability Implications of the Canadian Groundwater Resources under Changing Climate. *Sustainability* **2021**, *13*, 9778. https://doi.org/10.3390/su13179778.

3. Gregor, T.; Dressler, S.; Nierbauer, K.U.; Zizka, G. Loss of Plant Species Diversity in a Rural German Region-Assessment on Basis of a Historical Herbarium. *Tuexenia* **2016**, *36*, 191–204. https://doi.org/10.14471/2016.36.013.
4. Hussein, E.A.; Abd El-Ghani, M.M.; Hamdy, R.S.; Shalabi, L.E. Do Anthropogenic Activities Affect Floristic Diversity and Vegetation Structure More than Natural Soil Properties in Hyper-Arid Desert Environments? *Diversity* **2021**, *13*, 157. https://doi.org/10.3390/d13040157.
5. Jaric, I.; Roberts, D.L.; Gessner, J.; Solow, A.R.; Courchamp, F. Science Responses to IUCN Red Listing. *PeerJ* **2017**, *5*, e4025. https://doi.org/10.7717/peerj.4025.
6. Hegde, R.; Niranjana, K.; Srinivas, S.; Danorkar, B.A.; Singh, S.K. Site-Specific Land Resource Inventory for Scientific Planning of Sujala Watersheds in Karnataka. *Curr. Sci.* **2018**, *115*, 644–652. https://doi.org/10.18520/cs/v115/i4/644-652.
7. Pfeiffer, T.Z.; Maronic, D.S.; Zahirovic, V.; Stevic, F.; Zjalic, M.; Kajan, K.; Ozimec, S.; Mihaljevic, M. Early Spring Flora of the Sub-Pannonic Steppic Grassland (NATURA 2000 Site) in Bilje, Northeast Croatia. *Acta Bot. Croat.* **2016**, *75*, 157–163. https://doi.org/10.1515/botcro-2016-0029.
8. Wright, J.W.; Davies, K.F.; Lau, J.A.; McCall, A.C.; McKay, J.K. Experimental Verification of Ecological Niche Modeling in a Heterogeneous Environment. *Ecology* **2006**, *87*, 2433–2439. https://doi.org/10.1890/0012-9658(2006)87[2433:EVOENM]2.0.CO;2.
9. Radočaj, D.; Jurišić, M.; Gašparović, M.; Plaščak, I.; Antonić, O. Cropland Suitability Assessment Using Satellite-Based Biophysical Vegetation Properties and Machine Learning. *Agronomy* **2021**, *11*, 1620. https://doi.org/10.3390/agronomy11081620.
10. Nikolić, T.; Topić, J. *Croatian Red Book of Vascular Flora*; Ministry of Culture: Zagreb, Republic of Croatia, 2005.
11. Flora Croatica Database, Vascular Plants Taxonomy and Bibliography of Croatian Flora. Available online: https://hirc.botanic.hr/fcd/ (accessed on 20 April 2022).
12. Flora Croatica Database, Small Pasque Flower. Available online: https://hirc.botanic.hr/fcd/DetaljiFrame.aspx?IdVrste=8206&taxon=Pulsatilla+pratensis+(L.)+Miller+ssp.+nigricans+(St%C3%B6rck)+Zam (accessed on 19 April 2022).
13. Flora Croatica Database, Green-Winged Orchid. Available online: https://hirc.botanic.hr/fcd/DetaljiFrame.aspx?IdVrste=6997&taxon=Orchis+morio+L (accessed on 19 April 2022).
14. Flora Croatica Database, Hungarian False Leopardbane. Available online: https://hirc.botanic.hr/fcd/DetaljiFrame.aspx?IdVrste=27467&taxon=Doronicum+hungaricum+Rchb.+f (accessed on 19 April 2022).
15. Flora Croatica Database, Bloody Cranesbill. Available online: https://hirc.botanic.hr/fcd/DetaljiFrame.aspx?IdVrste=4812&taxon=Geranium+sanguineum+L (accessed on 19 April 2022).
16. Flora Croatica Database, Hungarian Iris. Available online: https://hirc.botanic.hr/fcd/DetaljiFrame.aspx?IdVrste=5437&taxon=Iris+variegata+L (accessed on 19 April 2022).
17. Taghizadeh-Mehrjardi, R.; Nabiollahi, K.; Rasoli, L.; Kerry, R.; Scholten, T. Land Suitability Assessment and Agricultural Production Sustainability Using Machine Learning Models. *Agronomy* **2020**, *10*, 573. https://doi.org/10.3390/agronomy10040573.
18. Bako, G.; Molnar, Z.; Bakk, L.; Horvath, F.; Feher, L.; Abram, O.; Morvai, E.; Biro, C.; Papay, G.; Furesz, A.; et al. Toward a High Spatial Resolution Aerial Monitoring Network for Nature Conservation-How Can Remote Sensing Help Protect Natural Areas? *Sustainability* **2021**, *13*, 8807. https://doi.org/10.3390/su13168807.
19. Zlinszky, A.; Heilmeier, H.; Balzter, H.; Czucz, B.; Pfeifer, N. Remote Sensing and GIS for Habitat Quality Monitoring: New Approaches and Future Research. *Remote Sens.* **2015**, *7*, 7987–7994. https://doi.org/10.3390/rs70607987.
20. Hallik, L.; Kuusk, A.; Lang, M.; Kuusk, J. Reflectance Properties of Hemiboreal Mixed Forest Canopies with Focus on Red Edge and Near Infrared Spectral Regions. *Remote Sens.* **2019**, *11*, 1717. https://doi.org/10.3390/rs11141717.
21. Rajah, P.; Odindi, J.; Mutanga, O. Evaluating the Potential of Freely Available Multispectral Remotely Sensed Imagery in Mapping American Bramble (*Rubus cuneifolius*). *S. Afr. Geogr. J.* **2018**, *100*, 291–307. https://doi.org/10.1080/03736245.2018.1461683.
22. Zhou, H.; Zhu, J.; Li, J.; Xu, Y.; Li, Q.; Yan, E.; Zhao, S.; Xiong, Y.; Mo, D. Opening a New Era of Investigating Unreachable Cliff Flora Using Smart UAVs. *Remote Sens. Ecol. Conserv.* **2021**, *7*, 638–648. https://doi.org/10.1002/rse2.214.
23. Casalegno, S.; Amatulli, G.; Bastrup-Birk, A.; Durrant, T.H.; Pekkarinen, A. Modelling and Mapping the Suitability of European Forest Formations at 1-Km Resolution. *Eur. J. For. Res.* **2011**, *130*, 971–981. https://doi.org/10.1007/s10342-011-0480-x.
24. Radočaj, D.; Jurišić, M.; Gašparović, M. A Wildfire Growth Prediction and Evaluation Approach Using Landsat and MODIS Data. *J. Environ. Manag.* **2022**, *304*, 114351. https://doi.org/10.1016/j.jenvman.2021.114351.
25. Awais, M.; Aslam, B.; Maqsoom, A.; Khalil, U.; Ullah, F.; Azam, S.; Imran, M. Assessing Nitrate Contamination Risks in Groundwater: A Machine Learning Approach. *Appl. Sci.* **2021**, *11*, 10034. https://doi.org/10.3390/app112110034.
26. Rodrigues, N.M.; Batista, J.E.; Mariano, P.; Fonseca, V.; Duarte, B.; Silva, S. Artificial Intelligence Meets Marine Ecotoxicology: Applying Deep Learning to Bio-Optical Data from Marine Diatoms Exposed to Legacy and Emerging Contaminants. *Biology* **2021**, *10*, 932. https://doi.org/10.3390/biology10090932.
27. Edalat, M.; Dastres, E.; Jahangiri, E.; Moayedi, G.; Zamani, A.; Pourghasemi, H.R.; Tiefenbacher, J.P. Spatial Mapping Zataria Multiflora Using Different Machine-Learning Algorithms. *Catena* **2022**, *212*, 106007. https://doi.org/10.1016/j.catena.2021.106007.
28. Zheng, C.; Wen, Z.; Liu, Y.; Guo, Q.; Jiang, Y.; Ren, H.; Fan, Y.; Yang, Y. Integrating Habitat Suitability and the Near-Nature Restoration Priorities into Revegetation Plans Based on Potential Vegetation Distribution. *Forests* **2021**, *12*, 218. https://doi.org/10.3390/f12020218.
29. Fois, M.; Cuena-Lombraña, A.; Fenu, G.; Bacchetta, G. Using Species Distribution Models at Local Scale to Guide the Search of Poorly Known Species: Review, Methodological Issues and Future Directions. *Ecol. Model.* **2018**, *385*, 124–132. https://doi.org/10.1016/j.ecolmodel.2018.07.018.

30. Republic of Croatia, State Geodetic Administration CROPOS Users' Manual. Available online: https://www.cropos.hr/files/docs/cropos_users-manual.pdf (accessed on 22 November 2021).
31. Hengl, T.; MacMillan, R.A. *Predictive Soil Mapping with R*; OpenGeoHub Foundation: Wageningen, The Netherlands, 2019; ISBN 978-0-359-30635-0.
32. Kim, D.; Kupfer, J.A. Tri-Variate Relationships among Vegetation, Soil, and Topography along Gradients of Fluvial Biogeomorphic Succession. *PLoS ONE* **2016**, *11*, e0163223. https://doi.org/10.1371/journal.pone.0163223.
33. Begert, M.; Frei, C. Long-Term Area-Mean Temperature Series for SwitzerlandCombining Homogenized Station Data and High Resolution Grid Data. *Int. J. Climatol.* **2018**, *38*, 2792–2807. https://doi.org/10.1002/joc.5460.
34. Conrad, O.; Bechtel, B.; Bock, M.; Dietrich, H.; Fischer, E.; Gerlitz, L.; Wehberg, J.; Wichmann, V.; Boehner, J. System for Automated Geoscientific Analyses (SAGA) v. 2.1.4. *Geosci. Model Dev.* **2015**, *8*, 1991–2007. https://doi.org/10.5194/gmd-8-1991-2015.
35. Maresma, A.; Ariza, M.; Martinez, E.; Lloveras, J.; Martinez-Casasnovas, J.A. Analysis of Vegetation Indices to Determine Nitrogen Application and Yield Prediction in Maize (*Zea mays* L.) from a Standard UAV Service. *Remote Sens.* **2016**, *8*, 973. https://doi.org/10.3390/rs8120973.
36. Rouse, J.; Haas, R.H.; Schell, J.A.; Deering, D.W. Monitoring Vegetation Systems in the Great Plains with ERTS. *NASA Spec. Publ.* **1974**, *351*, 309.
37. Barnes, E.M.; Clarke, T.R.; Richards, S.E.; Colaizzi, P.D.; Haberland, J.; Kostrzewski, M.; Waller, P.; Choi, C.; Riley, E.; Thompson, T.; et al. Coincident Detection of Crop Water Stress, Nitrogen Status and Canopy Density Using Ground-Based Multispectral Data. In Proceedings of the Fifth International Conference on Precision Agriculture, Bloomington, MN, USA, 16–19 July 2000; pp. 1–5.
38. Easterday, K.; Kislik, C.; Dawson, T.E.; Hogan, S.; Kelly, M. Remotely Sensed Water Limitation in Vegetation: Insights from an Experiment with Unmanned Aerial Vehicles (UAVs). *Remote Sens.* **2019**, *11*, 1853. https://doi.org/10.3390/rs11161853.
39. Csajbok, J.; Buday-Bodi, E.; Nagy, A.; Feher, Z.Z.; Tamas, A.; Virag, I.C.; Bojtor, C.; Forgacs, F.; Vad, A.M.; Kutasy, E. Multispectral Analysis of Small Plots Based on Field and Remote Sensing Surveys-A Comparative Evaluation. *Sustainability* **2022**, *14*, 3339. https://doi.org/10.3390/su14063339.
40. Blanco, V.; Jose Blaya-Ros, P.; Castillo, C.; Soto-Valles, F.; Torres-Sanchez, R.; Domingo, R. Potential of UAS-Based Remote Sensing for Estimating Tree Water Status and Yield in Sweet Cherry Trees. *Remote Sens.* **2020**, *12*, 2359. https://doi.org/10.3390/rs12152359.
41. Yue, L.; Wang, Y.; Wang, L.; Yao, S.; Cong, C.; Ren, L.; Zhang, B. Impacts of Soil Compaction and Historical Soybean Variety Growth on Soil Macropore Structure. *Soil Tillage Res.* **2021**, *214*, 105166. https://doi.org/10.1016/j.still.2021.105166.
42. Hengl, T.; Heuvelink, G.B.M.; Stein, A. A Generic Framework for Spatial Prediction of Soil Variables Based on Regression-Kriging. *Geoderma* **2004**, *120*, 75–93. https://doi.org/10.1016/j.geoderma.2003.08.018.
43. Radočaj, D.; Jug, I.; Vukadinović, V.; Jurišić, M.; Gašparović, M. The Effect of Soil Sampling Density and Spatial Autocorrelation on Interpolation Accuracy of Chemical Soil Properties in Arable Cropland. *Agronomy* **2021**, *11*, 2430. https://doi.org/10.3390/agronomy11122430.
44. Böhner, J.; Antonić, O. Chapter 8 Land-Surface Parameters Specific to Topo-Climatology. In *Developments in Soil Science*; Hengl, T., Reuter, H.I., Eds.; Geomorphometry; Elsevier: Amsterdam, The Netherlands, 2009; Volume 33, pp. 195–226.
45. Fan, B.; Tao, W.; Qin, G.; Hopkins, I.; Zhang, Y.; Wang, Q.; Lin, H.; Guo, L. Soil Micro-Climate Variation in Relation to Slope Aspect, Position, and Curvature in a Forested Catchment. *Agric. For. Meteorol.* **2020**, *290*, 107999. https://doi.org/10.1016/j.agrformet.2020.107999.
46. Kammer, P.M.; Schoeb, C.; Eberhard, G.; Gallina, R.; Meyer, R.; Tschanz, C. The Relationship between Soil Water Storage Capacity and Plant Species Diversity in High Alpine Vegetation. *Plant Ecol. Divers.* **2013**, *6*, 457–466. https://doi.org/10.1080/17550874.2013.783142.
47. Freeman, T.G. Calculating Catchment Area with Divergent Flow Based on a Regular Grid. *Comput. Geosci.* **1991**, *17*, 413–422. https://doi.org/10.1016/0098-3004(91)90048-I.
48. Johnson, B.G.; Thackray, G.D.; Van Kirk, R. The Effect of Topography, Latitude, and Lithology on Rock Glacier Distribution in the Lemhi Range, Central Idaho, USA. *Geomorphology* **2007**, *91*, 38–50. https://doi.org/10.1016/j.geomorph.2007.01.023.
49. Kuhn, M. Building Predictive Models in R Using the Caret Package. *J. Stat. Softw.* **2008**, *28*, 1–26.
50. Ogola, H.J.O.; Selvarajan, R.; Tekere, M. Local Geomorphological Gradients and Land Use Patterns Play Key Role on the Soil Bacterial Community Diversity and Dynamics in the Highly Endemic Indigenous Afrotemperate Coastal Scarp Forest Biome. *Front. Microbiol.* **2021**, *12*, 592725. https://doi.org/10.3389/fmicb.2021.592725.
51. Kurtz, B.C.; Souza, V.C.; Magalhaes, A.M.; de Paula-Souza, J.; Duarte, A.R.; Joaquim, G.O. The Vascular Flora and Vegetation of Queimada Grande Island, Sao Paulo State, Southeastern Brazil. *Biota Neotrop.* **2017**, *17*, e20170336. https://doi.org/10.1590/1676-0611-BN-2017-0336.
52. Campos, V.E.; Gatica, G.; Bellis, L.M. Remote Sensing Variables as Predictors of Habitat Suitability of the Viscacha Rat (*Octomys mimax*), a Rock-Dwelling Mammal Living in a Desert Environment. *Mammal. Res.* **2015**, *60*, 117–126. https://doi.org/10.1007/s13364-015-0215-3.
53. Fish, A. Crash Theory: Entrapments of Conservation Drones and Endangered Megafauna. *Sci. Technol. Hum. Values* **2021**, *46*, 425–451. https://doi.org/10.1177/0162243920920356.

54. De Deyn, G.B.; Raaijmakers, C.E.; Zoomer, H.R.; Berg, M.P.; de Ruiter, P.C.; Verhoef, H.A.; Bezemer, T.M.; van der Putten, W.H. Soil Invertebrate Fauna Enhances Grassland Succession and Diversity. *Nature* **2003**, *422*, 711–713. https://doi.org/10.1038/nature01548.
55. Luft, L.; Neumann, C.; Freude, M.; Blaum, N.; Jeltsch, F. Hyperspectral Modeling of Ecological Indicators—A New Approach for Monitoring Former Military Training Areas. *Ecol. Indic.* **2014**, *46*, 264–285. https://doi.org/10.1016/j.ecolind.2014.06.025.
56. Li, Q.; Wong, F.K.K.; Fung, T. Mapping Multi-Layered Mangroves from Multispectral, Hyperspectral, and LiDAR Data. *Remote Sens. Environ.* **2021**, *258*, 112403. https://doi.org/10.1016/j.rse.2021.112403.
57. Saad, F.; Biswas, S.; Huang, Q.; Corte, A.P.D.; Coraiola, M.; Macey, S.; Carlucci, M.B.; Leimgruber, P. Detectability of the Critically Endangered Araucaria Angustifolia Tree Using Worldview-2 Images, Google Earth Engine and UAV-LiDAR. *Land* **2021**, *10*, 1316. https://doi.org/10.3390/land10121316.
58. Rominger, K.; Meyer, S.E. Application of UAV-Based Methodology for Census of an Endangered Plant Species in a Fragile Habitat. *Remote Sens.* **2019**, *11*, 719. https://doi.org/10.3390/rs11060719.
59. Wylie, B.K.; Pastick, N.J.; Picotte, J.J.; Deering, C.A. Geospatial Data Mining for Digital Raster Mapping. *GIScience Remote Sens.* **2019**, *56*, 406–429. https://doi.org/10.1080/15481603.2018.1517445.
60. Leduc, M.-B.; Knudby, A.J. Mapping Wild Leek through the Forest Canopy Using a UAV. *Remote Sens.* **2018**, *10*, 70. https://doi.org/10.3390/rs10010070.
61. Radočaj, D.; Obhođaš, J.; Jurišić, M.; Gašparović, M. Global Open Data Remote Sensing Satellite Missions for Land Monitoring and Conservation: A Review. *Land* **2020**, *9*, 402. https://doi.org/10.3390/land9110402.
62. Eugenio Abrego, M.; Acuna-Perales, N.; Alfaro-Shigueto, J.; Azocar, J.; Barragan Rocha, A.R.; Baquero, A.; Cotto, A.; Darquea, J.; de Paz, N.; Donoso, M.; et al. Enhanced, Coordinated Conservation Efforts Required to Avoid Extinction of Critically Endangered Eastern Pacific Leatherback Turtles. *Sci. Rep.* **2020**, *10*, 4772. https://doi.org/10.1038/s41598-020-60581-7.
63. Warner, K.; Zommers, Z.; Wreford, A.; Hurlbert, M.; Viner, D.; Scantlan, J.; Halsey, K.; Halsey, K.; Tamang, C. Characteristics of Transformational Adaptation in Climate-Land-Society Interactions. *Sustainability* **2019**, *11*, 356. https://doi.org/10.3390/su11020356.